Design of Exponantial-2-DOF-PID Controller Using Stochastic Fractal Search Algorithm for Interconnected Electric Power Systems

Mehmet KARAYEL*‡

* Department of Electrical and Energy, Vocational School, Çankırı Karatekin University, Çankırı, Turkey,

(mkarayel@karatekin.edu.tr)

‡Corresponding Author; Mehmet KARAYEL, Department of Electrical and Energy, Vocational School, Çankırı Karatekin University, Çankırı, Turkey, mkarayel@karatekin.edu.tr

Received: 15.05.2025 Accepted:10.06.2025

Abstract- To meet the increasing energy demand, it is an inevitable necessity to connect alternative energy sources and different energy sources to the interconnected power system. The most important factor determining the quality and reliability of energy in the interconnected power system is frequency. Load changes, external disturbances and parameter changes in the power system (PS) cause changes in frequency and power values in all areas connected to the power system. Fast and reliable control of power and frequency changes occurring in a power system is called load frequency control (LFC). For good quality and reliable energy production, the LFC must be resilient to unknown external disturbances and parameter changes in the power system. To this end, this research presents an exponential two degrees of freedom PID (EXP-2DOF-PID) controller to improve the LFC performance of PSs. The proposed controller consists of a tunable exponential function placed in front of a two degree of freedom PID controller. The exponential function produces a nonlinear output signal by acting on the error value at its input and the derivative of the error. To achieve the highest performance, the parameters of the proposed controller are determined by the stochastic fractal search (SFS) algorithm. The Integral of Time Absolute Error (ITAE) cost function was used during the optimization. The EXP-2DOF-PID controller has been tested on different PS models to verify its performance and versatility. Extensive comparison is made to highlight the performance of the proposed controller. All the simulations performed for this research are modelled in a MATLAB/m-file script and the results are plotted using MATLAB R2020b.

Keywords Load frequency control, exponential, 2DOF-PID, stochastic fractal search algorithm, optimization.

1. Introduction

With the increasing population and the development of industry in the world, the need for energy and the complexity of power systems are increasing day by day. The fundamental objective of a power system is to consistently supply consumers with secure and stable electrical energy. The stability and dependability of the power system can be maintained through the continuous provision of high-quality and uninterrupted electric power. Frequency stability in power systems serves as a key indicator of overall power quality. Load Frequency Control (LFC) is a critical technology used to sustain power equilibrium, ensure frequency steadiness, and maintain power quality. The primary aim of LFC is to regulate generation frequency and respond to load variations in interconnected power networks, ensuring that both system frequency and tie-line power remain at their nominal levels, whether under normal operating conditions or during significant load fluctuations. LFC technology is vital to maintaining power equilibrium, stable frequency, and high-quality power delivery. The main purpose of LFC is to regulate generation frequency and load change in interconnected power systems. while also maintaining system frequency and tie-line power at their nominal levels, regardless of normal operating conditions or significant load fluctuations [1-3]. Beyond mitigating load disturbances, the LFC must exhibit strong robustness to withstand uncertainties in system parameters and the randomness of load variations. Consequently, an effective, resilient, and fast-responding LFC controller is essential to achieve optimal performance in today's complex power systems.

In recent years, numerous studies in the literature have extensively explored LFC strategies to enhance the operational efficiency of interconnected power systems. In current research on LFC, PI/PID controller structure is still a much-preferred controller due to its simplicity, low cost and many other advantages, and design of the controller and choice of its parameters are crucial factors that significantly influence the effectiveness of LFC [5-7]. In [8,9], PSO algorithm-based PI/PID controller was used for multi-source PSs with renewable energy sources. In [10], Harris Hawks optimizer (HHO) algorithm-based PI controller was introduced in multi-source PSs with renewable energy sources. In [11], modified stochastic fractal search (ISFS) algorithm was used to find PID controller parameters in three-different PSs of different manufacturing plants. An EXP-PID controller using the snake optimization algorithm for frequency regulation in various multi-source PSs was introduced in [12] and a PI/PID controller tuned with a modified gray wolf optimizer (GWO) algorithm was introduced in [13]. In [14], a PID controller optimized using the Differential Evolution (DE) algorithm was introduced to determine the optimal parameter settings for the Automatic Generation Control (AGC) in an interconnected power grid.

Despite the positive results obtained above, researchers continue to search for effective techniques. In this line of research, numerous studies are being conducted to overcome the limitations of conventional PID controllers or to enhance their structure in order to achieve improved performance. In [15], presents a novel control strategy for a first-order plus time-delay (FOPTD) system, applied to a deregulated multi-area power system (MAPS), termed the FUZZY-(1+PD)-FOPID controller. For frequency regulation in multi-area PSs with different sources, DSA based cascade (1+PD)-PID controller was proposed in [16] and FOPI-FOPD controller was proposed in [17]. In [18], the nonlinear nature of the governor dead band (GDB) in PSs was evaluated using a 2-DOF-PID controller based on the DE algorithm for a two-area PS with a GDB. In [19], a 2DOF(PI)-PDF mechanism based on opposition-based volleyball premier league (OVPL) algorithm was introduced for two-area thermal and hydroelectric PS equipped with GDB. In [20], proposes a PD-(1+II) controller designed using the Rime Optimization Algorithm (RIME) to enhance both frequency and voltage stability in a 2-area thermal PS.

In section-2, details the power systems used for research. Then, in section-3, the modeling of the proposed EXP-2DOF-PID controller and the Stochastic fractal search algorithm are introduced. In Section 4, the simulation results of the proposed study are presented in detail and compared with similar studies. In Section 5, State Space Model of 2-ANRT PS is presented. Finally, in section-5 the observations of the study presented in the paper are concluded.

2. Description and Modeling of Interconnected PS

2.1. 2-Area Non-Reheat Thermal (2-ANRT) PS

Initially, a 2-ANRT PS model interconnected through a tie-line is used to effectiveness of the proposed controller, as illustrated in Fig. 2. Each area consists of a thermal production facility consisting of a non-reheat turbine and speed governor with the same capacity. The parameters of this system are listed in "Appendix". In the literature, this model has often been preferred by researchers to evaluate LFC approaches [21-23]. In Fig 1, illustrate single-line diagram of 2-ANRT PS model.

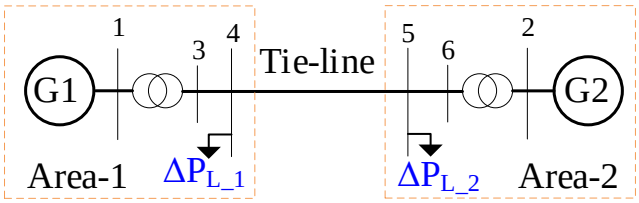

Fig. 1. Single-line diagram of 2-ANRT PS.

The secondary controller in each area produces an area control error (ACE) control signal that weights the tie-line power and frequency deviations by a B factor. This control signal guarantees that the frequency and tie-line power flow stay within specified boundaries. When a load variation occurs in the PS, the Area Control Error (ACE) shifts away from zero and must be rapidly corrected to return to zero. Therefore, it requires the secondary controller to be efficient and high-performance. The speed governor is represented in a linear form in Fig. 2(a). In Fig. 2(b), the model is revised to include the effect of the GDB nonlinearity to obtain more realistic results.

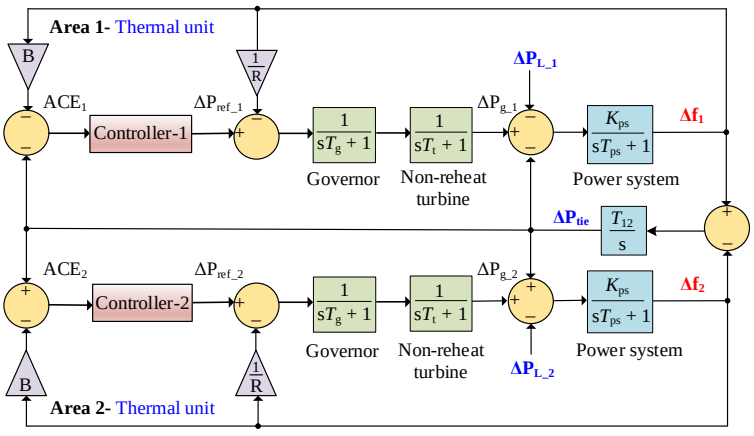

(a)

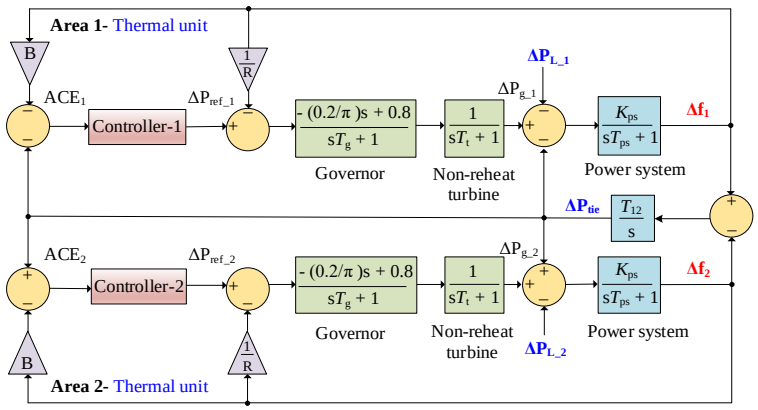

(b)

Fig. 2. Transfer function model of *2-ANRT* PS (a) no GDB (b) with GDB.

It is assumed that the GDB valve positions remain the same at all speed changes, causing oscillations in the system.

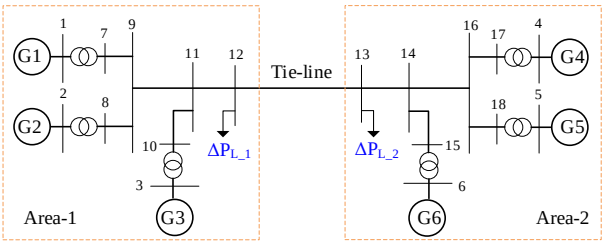

Fig. 3. Single-line diagram of 2-AMS PS.

As a result, the frequency deviations in both areas as system outputs are calculated as follows.

$$\Delta f_i(s) = G_{ps}(s)\left[\Delta P_{t\_i}(s) - \Delta P_{L\_i}(s)\Delta P_{tie}\right], \text{ i=1, 2} \quad (1)$$

Power exchange across the tie-line flowing between interconnected control areas.

$$\Delta P_{tie} = \frac{T_{12}}{s}[\Delta f_1 - \Delta f_2] \quad (2)$$

Where, T_{12} is synchronization coefficient. The signal equations for A and B are as follows. It is essential to ensure that the standard deviation of these signals remains zero

$$ACE_1 = -B\Delta f_1 - \Delta P_{tie} \quad (3)$$
$$ACE_2 = -B\Delta f_2 - \Delta P_{tie} \quad (4)$$

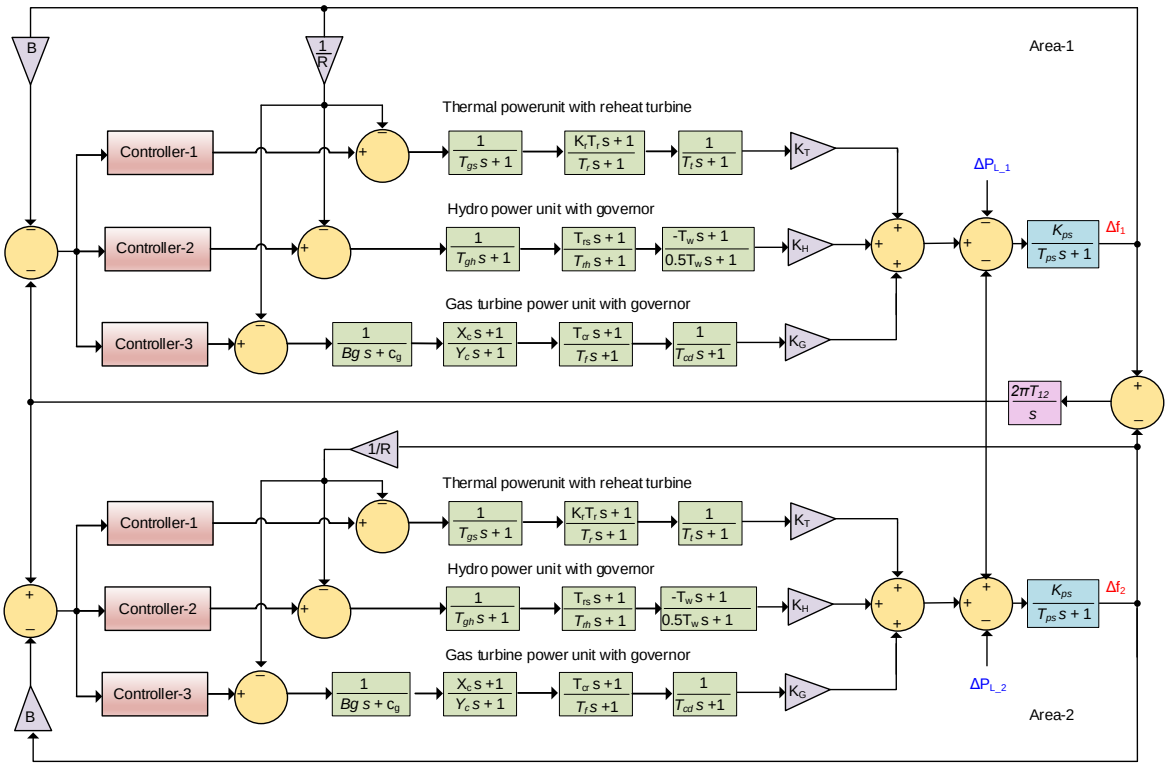

Fig. 4. T.F. model of 2-AMS PS.

2.2. 2-Area Multi-Source (2-AMS) Power System

The 2-AMS PS model is developed to evaluate the versatility and controlling capacity of the proposed controller. In this TF model, there are three different power plants in each area, namely reheat thermal power plant, hydroelectric power unit and gas turbine power unit, as illustrated in Fig. 4. To rigorously evaluate the dynamic performance of the EXP-2DOF-PID controller, two power system areas incorporating distinct generating units are interconnected via a tie-line. Additionally, a participation factor (K_T, K_H, K_G) is included to determine the contribution of each power plant to the total generation. The parameters of this system are listed in "Appendix". In Fig 3, illustrate single-line diagram of 2-AMS PS.

3. The Proposed Controller Strategy

3.1. EXP-2DOF-PID

The proposed EXP-2DOF-PID controller is given in Fig. 5. As can be seen, the exponential block is placed in front of the 2DOF-PID block, and they work in a cascade manner. Here, the exponential block acts as a variable gain ($\sigma(t)$). The error signal $e(t)$ from the system and its time derivative are passed through two exponential functions and then nonlinearly combined to produce $\sigma(t)$ [12]. In 2DOF-PID controller block, there are two control loops. The two control loops have two inputs, the Reference signal ($\sigma(t)$) and the variation of frequency (Δf), which is the output signal of the system. to the 2DOF-PID controller includes two weight parameters (P_w,D_w) that help to improve its performance. The output signal is included in the controller to expand the working area instead of two points as in traditional PID controllers [24]. $\sigma(t)$ is then input to the 2DOF-PID controller block to obtain the final output signal $\Delta u_{EXP-2DOF-PID}$ signal.

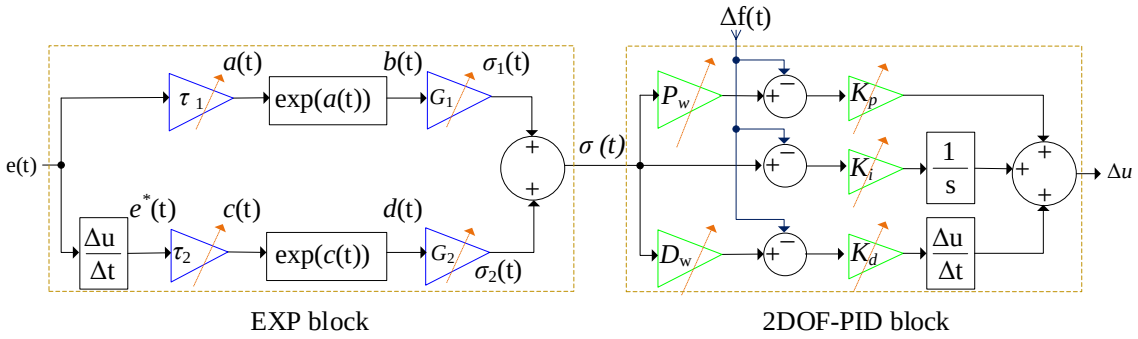

Fig. 5. The configuration of EXP-2DOF-PID.

The most important element in the EXP block is the nonlinear transformation from the error $e(t)$ and its time derivative $e^*(t)$ to $\sigma(t)$. For this purpose, two exponential functions given in Eq. (5) are considered.

$$\sigma_1(t) = G1\left(\frac{2}{1+e^{-\tau_1 e(t)}} - 1\right)$$
$$\sigma_2(t) = G2\left(\frac{2}{1+e^{-\tau_2 \dot{e}(t)}} - 1\right) \quad (5)$$

Where, τ_1, τ_2, G_1, and G_2 are variable parameters that characterize the exponential function to achieve better performance. Here, $G_{1,2}$ represents the upper bound of the function, $\tau_{1,2}$ allows obtaining exponential functions with different steepnesses.

The output of the EXP-2DOF-PID controller is given in Eq. (6).

$$\Delta u(t) = K_p(t)\left(P_w.\sigma(t) - \Delta f(t)\right) + K_i(t)\int_0^t\left(\sigma(t) - \Delta f(t)\right)dt + K_d\,\frac{d\left(D_w.\sigma(t) - \Delta f(t)\right)}{dt} \quad (6)$$

Where K_p, K_i, K_d are gain of PID parameters, P_w denotes the reference weight for the proportional gain, D_w represents the weight to the derivative, $\sigma(t)$ is a nonlinear expression of error signal $e(t)$ and $\sigma(t) = \sigma_1(t) + \sigma_2(t)$ and $\Delta f(t)$ is the variation of frequency.

3.2. Stochastic Fractal Search (SFS) Algorithm

The stochastic fractal search algorithm is a powerful meta-heuristic optimization algorithm inspired by the natural phenomena of growth. To find the best server, this method mimics the fractal property. Here, the two main components of SFS's search for the best solution are the diffusion and update processes. In the diffusion process, it increases the probability of finding the best solution and reaching the global optimum rather than staying at the optimum value of the current position. In the update process, the positions of the points in the group are updated based on the positions of other points in the search group [25]. Fundamental processes of SFS algorithm in Fig. 6.

In the initially, P particle population which is initialized randomly within the boundaries specified by the problem's lower (LB) and upper (UB) constraints.

$$P = LB + \varepsilon \times (UB - LB) \quad (7)$$

Where ε is represents a randomly selected value between 0 and 1. During the diffusion phase, the Gaussian Walk statistical method is applied to produce new particles across all populations, as described in Eq. (8) and Eq. (9).

Diffusion process is conducted for each point in the population. Subsequently, only the optimal position resulting from diffusion is retained for each point, others are ignored.

$$GW_1 = Gauss(\mu_{BP}, \sigma) + (\varepsilon \times BP - \varepsilon' \times P_i) \quad (8)$$

$$GW_2 = Gauss(\mu_{BP}, \sigma) \quad (9)$$

Where, ε and ε′ are represent a randomly selected value between 0 and 1. BP and P_i are position of the best point and i-th point in the population, respectively. μ_{BP} and σ are that generate random number, a mean and standard deviation parameter in the Gaussian Walk function, respectively.

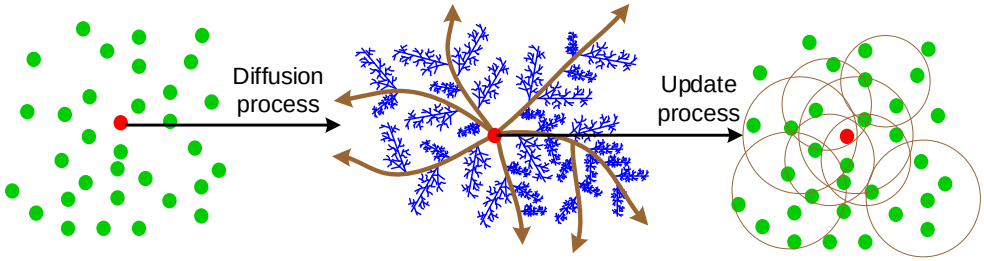

Fig. 6. Main processes of SFS algorithm.

Standard deviation parameter (σ) is calculated as a Eq. (10).

$$\sigma = \frac{log(g)}{g} \times |P_i - BP| \quad (10)$$

Where, the generation number (g) of the $\frac{log(g)}{g}$ term approaches zero as its elements increase, thus reducing the size of the Gaussian jumps to approach the solution. In the next step, the initial phase of exploration involves performing two sequential updates. In the first update process, particles are ranked according to their fitness value. Then, each particle i is given a probability value as in Eq. (11).

$$Pa_i = \frac{rank(P_i)}{N} \quad (11)$$

Where, N indicates the total number of particles within the group, Pa_i is the probability value calculated based on the ranking of a particle among others. This equation determines the probability of particles based on their fitness values. In the first update phase, for all of point P_i in the group, if Pa_i is smaller than a randomly generated number (ε), the j-th component of P_i is updated according to Eq.(12), otherwise it remains unchanged.

$$P_i'(j) = P_x(j) - \varepsilon \times \left(P_y(j) - P_i(j)\right) \quad (12)$$

Where, P_i' is the new modified component of P_i, P_x and P_y are randomly chosen points in the group, ε represent a randomly selected value between 0 and 1. All points obtained as a result of the first update process are re-ranked using Eq.5 and then the second update process begins. As before, if the condition $Pa_i < \varepsilon$ is satisfied, a new point is replaced for P_i' using Eq. (13), otherwise it remains unchanged.

$$P_i' = P_i - \varepsilon \times (P_x - BP) | \varepsilon' \leq 0.5$$
$$P_i' = P_i - \varepsilon \times \left(P_x - P_y\right) | \varepsilon' > 0.5 \quad (13)$$

In order to obtain a more effective transient response to frequency regulation depending on the power change in the LFC system, the optimum values for τ_1, τ_2, G_1, G_2, K_p, K_i, K_d, W_p, W_d parameters of the proposed EXP-2DOF-PID controller were tried to be searched by using the SFS algorithm. To test the robustness of the proposed controller, it was applied to different hybrid power systems separately and it was seen that the control performance of the system was effectively increased. Pseudo code of SFS algorithm is given in Algorithm 1.

Algorithm 1. Pseudo code of SFS

```
Initialize a population with random particles
while  t < maximum generation number
  % Diffision Process
  for each particle P_i in the group
      for k = 1:maximum number of diffision
        Diffuse P_i based on Gaussian Walks to some
        particles to be generated. Eq.(2) and Eq. (3)
      end
  end
  % Update First Process
  First, all points are ranked based on Eq.(5)
  For each particle P_i in the group
      if  rand(0,1) > Pa_i
        Calculate and update particle P_i by Eq.(6)
      end
  end
  % Update Second Process
  Once again, all points obtained by the first update
  process are ranked based on Eq.(5).
  for each particle P_i' in the group
      if  rand(0,1) > Pa_i'
        Update position based on Eq.(7)
      end
  end
t = t + 1
end
```

There are four types of performance criteria in determining the optimization-based controller parameters. These are IAE, ISE, ITSE and ITAE. In the literature, ISE and ITAE criteria are commonly used due to their better performance in LFC studies. ITAE cost function gives faster results than ISE in power systems due to its time-weighted structure, fast recovery of long-term faults, short settling time and better damping of oscillations [26]. Therefore, ITAE was preferred as the cost function in this study.

In this study, ITAE was preferred as the objective function. With the smallest value of the ITAE function, the control response of the power and frequency changes that settle at 0 pu value in the shortest time was tried to be obtained. The EXP-2DOF-PID controller design was tried to solve as a constrained optimization problem. Therefore, ITAE value is minimized by considering the inequalities in Eq. (14).

$$\tau_1^{min} \le \tau_1^* \le \tau_1^{max}, \quad \tau_2^{min} \le \tau_2^* \le \tau_2^{max},$$
$$G_1^{min} \le G_1^* \le G_1^{max}, \quad G_2^{min} \le G_2^* \le G_2^{max}, \qquad (14)$$
$$K_p^{min} \le K_p^* \le K_p^{max}, \quad K_i^{min} \le K_i^* \le K_i^{max},$$
$$K_i^{min} \le K_i^* \le K_i^{max}, \quad K_d^{min} \le K_d^* \le K_d^{max},$$
$$W_p^{min} \le W_p^* \le W_p^{max}, \quad W_d^{min} \le W_d^* \le W_d^{max}$$

Where, min and max represent the lower and upper limits of the controller parameters. In this study, the controller parameter bounds were chosen as [0, 2] for τ_1-τ_2, and [0, 5] for the others parameters, in accordance with ranges commonly adopted in the literature [12], [18], [21], [27–29]. After the optimization process, the values of τ_1^*, τ_2^*, G_1^*, G_2^*, K_p^*, K_i^*, K_d^*, W_p^*, W_d^* which give the minimum value of the ITAE cost function, were taken as the most appropriate values of the controller parameters and used in simulation studies.

4. Simulation Results

Initially, the effectiveness of the proposed EXP-2DOF-PID controller is evaluated using a 2-ANRT PS model that excludes the GDB. Throughout the simulation, a load disturbance of 0.1 per unit is introduced in Area 1 at $t_s = 0\ s$.

Table 1. Comparative performance analysis in term of controller parameters and t_s/J_{ITAE} for 2-ANRT PS, excluding GDB**.**

Algorithm		TLBO: 2DOF PID [27]	hPSO-PS: fuzzy PID[28]	ISFS: PID[21]	DSA: FOPID[18]	DSA: FOPI-FOPD[18]	SFS: EXP-2DOF-PID [proposed]
Parameters		$K_p = 1.892$ $K_i = 1.747$ $K_d = 0.226$ $N = 112.82$ $W_p = 0.483$ $W_d = 1.120$	$K_2 = 0.985$ $K_2 = 0.559$ $K_p = 0.993$ $K_i = 0.720$	$K_p = 1.629$ $K_i = 2.00$ $K_d = 0.588$	$K_p = 1.248$ $K_i = 2.999$ $K_d = 3.00$ $\lambda = 1.100$ $\mu = 0.631$	$K_{p1} = 1.248$ $K_{p2} = 2.999$ $K_i = 2.999$ $K_d = 3.00$ $\lambda = 1.100$ $\mu = 0.631$	$\tau_1 = 1.871$ $G_1 = 4.862$ $\tau_2 = 1.925$ $G_2 = 1.839$ $K_p = 0.827$ $K_i = 4.896$ $K_d = 0.009$ $W_p = 1.541$ $W_d = 2.879$
t_s **(s) (2% band)**	Δf_1	2.41	2.26	2.15	1.13	0.72	**0.44**
	Δf_2	2.13	3.74	3.66	2.73	1.78	**1.69**
	ΔP_{tie}	2.56	2.94	3.01	2.23	0.86	**0.57**
J_{ITAE}		0.0269	0.1438	n/r	0.0778	0.0180	**0.0080**

The performance response of the proposed controller is compared with recent studies under the same conditions in Table 1. It is seen that the j_{ITAE} of the responsesΔf_1, Δf_2 and ΔP_{tie} are minimized with the proposed controller and its value is 8E-03. The proposed controller achieves settling times of 0.44 s, 1.69 s, and 0.572 s, which are the lowest among others.

In Fig. 7, the frequency and tie-line responses are shown comparatively in a 2-ANRT PS, excluding GDB. It is clear that the proposed EXP-2DOF-PID controller exhibits a small initial undershoot when responding to a 0.1 pu load change but swiftly stabilizes at zero without oscillations.

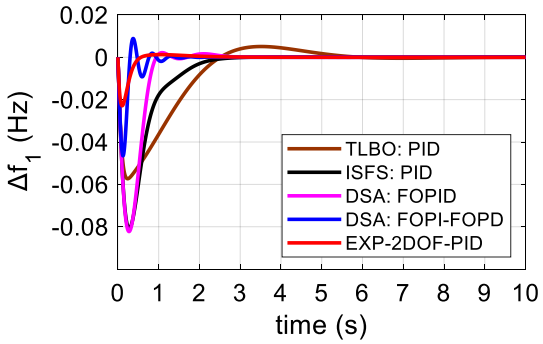

(a)

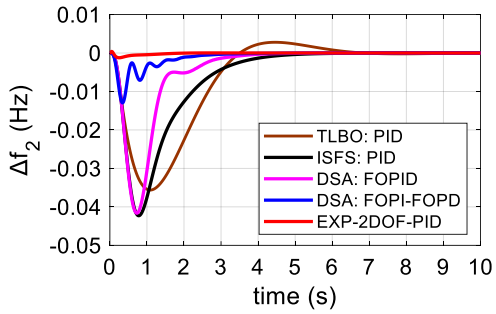

(b)

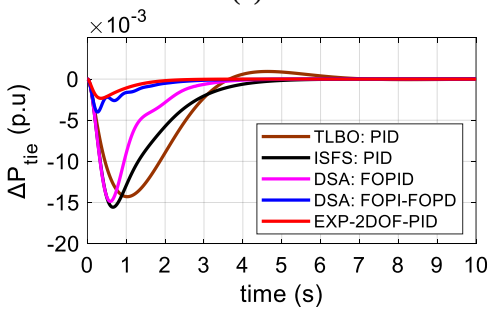

(c)

Fig. 7. Responses comparison for 2-ANRT PS excluding GDB (a) Δf_1 (b) Δf_2 (c) ΔP_{tie}.

In Table 2 presents the optimization simulation results when the system is 2-ANRT PS with GDB nonlinearity and a load variation of 0.01 pu is applied to area-1 at $t_s = 0\ s$. The results obtained were compared with published studies under the same conditions. Considering the error rates in Table 2, As seen that the proposed scheme outperforms all its competitors. . j_{ITAE} value is 19E-03 and Settlement times are $\Delta f_1 = 0.5s$, $\Delta f_2 = 1.35s$ and $\Delta P_{tie} = 1.02s$.

The comparison of system responses of 2-ANRT PS with GDB is given in Fig. 8. As clearly seen that by including the nonlinearity with GDB, there are oscillations in the responses of other studies but the proposed controller is least affected. After the initial drop, the responses of Δf_1, Δf_2 and ΔP_{tie} stabilize at zero in a short time using the proposed approach.

Finally, the optimized controller parameters of proposed and published similar works for 2-AMS PS are given in Table 3. All the results given in Table 3 were obtained by applying a 0.02 pu load change to area-1 at, $t_s = 0\ s$. Examining the results in the table, the SFS tuned EXP-2DOF-PID controller parameters can be obtained as effectively as possible, which makes it possible to minimize j_{ITAE}.(0.02237).

Table 2. Comparative performance analysis in term of controller parameters and t_s/J_{ITAE} for 2-ANRT PS with GDB**.**

Algorithm		**DE: PID [29]**	**ISFS: PID[21]**	**DSA: FOPID[18]**	**DSA: FOPI-FOPD[18]**	**SFS: EXP-2DOF-PID [proposed]**
Parameters		$K_p = 0.238$	$K_p = 0.389$	$K_p = 2.557$	$K_{p1} = 2.318$	$\tau_1 = 1.491$
		$K_i = 0.971$	$K_i = 1.011$	$K_i = 2.999$	$K_{p2} = 2.999$	$G_1 = 3.751$
		$K_d = 0.492$	$K_d = 0.769$	$K_d = 0.793$	$K_i = 2.987$	$\tau_2 = 0.703$
				$\lambda = 1.002$	$K_d = 0.439$	$G_2 = 1.020$
				$\mu = 1.251$	$\lambda = 1.000$	$K_p = 2.586$
					$\mu = 1.464$	$K_i = 4.129$
						$K_d = 1.561$
						$W_p = 1.018$
						$W_d = 0.459$
t_s **(s)**	Δf_1	6.87	6.25	2.34	1.22	**0.50**
(2% band)	Δf_2	6.89	6.48	3.63	2.25	**1.35**
	ΔP_{tie}	4.40	4.40	2.33	1.05	**1.02**
J_{ITAE}		n/r	n/r	0.0121	0.0034	**0.0019**

Additionally, the proposed method has less settling time than other compared studies. $\Delta f_1 = 2.18$, $\Delta f_2 = 3.48s$ and $\Delta P_{tie} = 1.98s$.

In Fig. 9, frequency and tie-line responses are compared for the 2-AMS PS. When Fig. 9 is examined, as seen that the responses with the SFS optimized EXP-2DOF-PID controller are faster, do not include oscillations, and are more effective than the others.

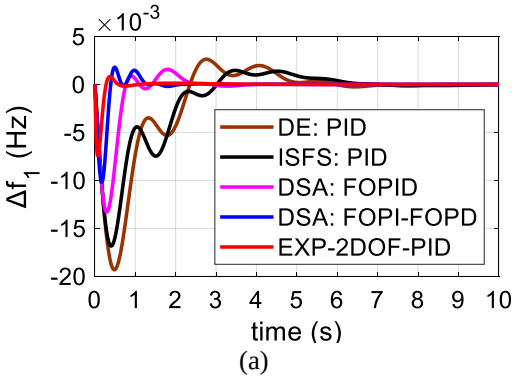

(a)

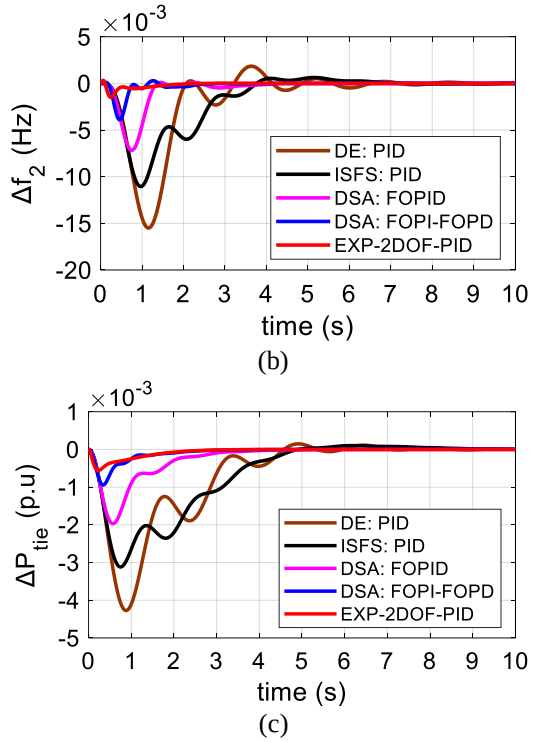

Fig. 8. Responses comparison for 2-ANRT PS with GDB (a) Δf_1 (b) Δf_2 (c) ΔP_{tie}.

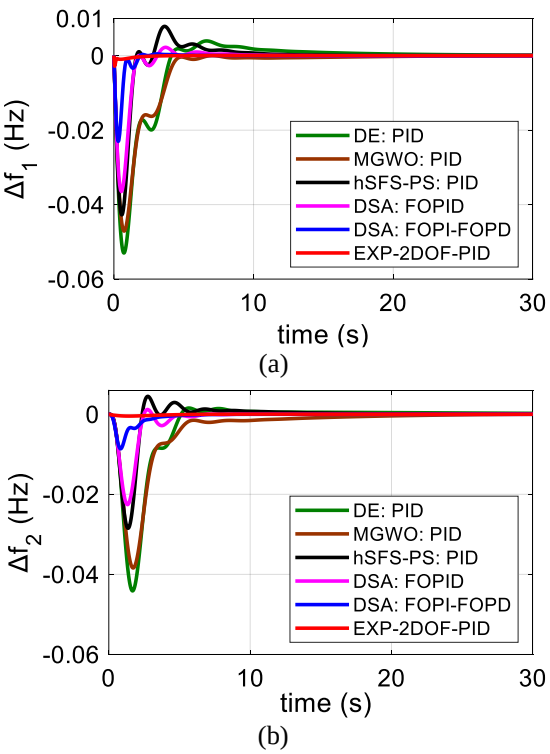

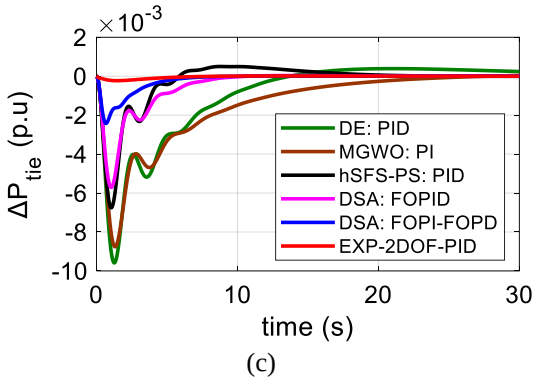

Fig. 9. Responses comparison for 2-AMS PS (a) Δf_1 (b) Δf_2 (c) ΔP_{tie}.

In conclusion, the system is tested with random load variations to assess the stability and robustness of the EXP-2DOF-PID controller optimized using the SFS algorithm. For this purpose, 2-ANRT power system has been designated as the test model. The controller's parameters, provided in Table 1, remain fixed and are not adjusted to respond to the updated system state. Throughout simulation, load variations are applied to all areas as in Fig. 10. As illustrated, load variations have complex properties that change continuously and instantaneously.

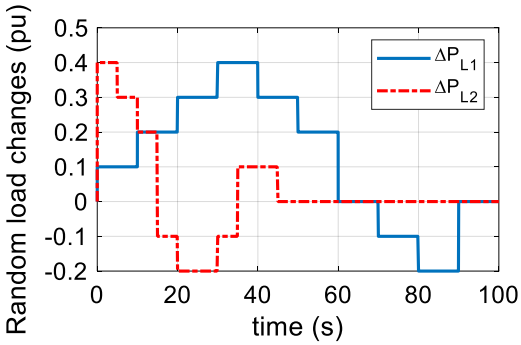

Fig. 10. Random load variation.

Fig. 11 illustrates the frequency and tie-line responses under random load variations. As can be seen in Fig. 11(a), frequency control remains effective. Sudden load changes that are quickly handled show a good response, similar to the first one. Also, it should be emphasized in Fig. 11(b) that ΔP_{tie} rapidly and steadily returns to zero following every load change. In conclusion, we can state that the proposed SFS tuned EXP-2DOF-PID controller design shows excellent performance by achieving good distortion rejection without changing the parameters.

Table 3. Comparative performance analysis in term of controller parameters and t_s/J_{ITAE} for 2-AMS PS**.**

Algorithm		**DE: PI [30]**	**MGWO: PID [31]**	**hSFS-PS: PID [32]**	**DSA: FOPID[18]**	**DSA: FOPI-FOPD[18]**	**SFS: EXP-2DOF-PID [proposed]**
Parameters		Unit1: $K_p = 0.779$ $K_i = 0.276$ $K_d = 0.689$ Unit2: $K_p = 0.580$ $K_i = 0.229$ $K_d = 0.708$ Unit3: $K_p = 0.502$ $K_i = 0.953$ $K_d = 0.657$	Unit1: $K_p = 1.750$ $K_i = -0.009$ $K_d = 0.750$ Unit2: $K_p = 0.311$ $K_i = 0.310$ $K_d = 0.003$ Unit3: $K_p = 0.009$ $K_i = 1.241$ $K_d = 0.690$	Unit1: $K_p = -1.707$ $K_i = -1.959$ $K_d = -1393$ Unit2: $K_p = -0.745$ $K_i = 0.137$ $K_d = -0.990$ Unit3: $K_p = -1.825$ $K_i = -1.681$ $K_d = -0.163$	Unit1 $K_p = 1.999$ $K_i = 2.000$ $K_d = 1.999$ $\lambda = 0.502$ $\mu = 0.239$ Unit2: $K_p = 1.203$ $K_i = 1.191$ $K_d = -0.437$ $\lambda = 0.507$ $\mu = 0.375$ Unit3: $K_p = 0.927$ $K_i = 2$ $K_d = 1.999$ $\lambda = 1.210$ $\mu = 1.268$	Unit1 $K_{p1} = -2$ $K_{p2} = -2$ $K_i = -2$ $K_d = -2$ $\lambda = 0.504$ $\mu = 0.010$ Unit2: $K_{p1} = 1.743$ $K_{p2} = -2$ $K_i = -2$ $K_d = -1.363$ $\lambda = 0.951$ $\mu = 0.088$ Unit3: $K_{p1} = -2$ $K_{p2} = -1.781$ $K_i = -2$ $K_d = -2$ $\lambda = 0.869$ $\mu = 1.2$	Unit1: $\tau_1 = 1.986$ $G_1 = 4.999$ $\tau_2 = 0.227$ $G_2 = 2.614$ $K_p = 4.777$ $K_i = 4.698$ $K_d = 4.434$ $W_p = 4.942$ $W_d = 0.763$ Unit2: $\tau_1 = 0.867$ $G_1 = 3.315$ $\tau_2 = 0.088$ $G_2 = 3.227$ $K_p = 3.820$ $K_i = 1.257$ $K_d = 0.200$ $W_p = 1.449$ $W_d = 0.176$ Unit3: $\tau_1 = 1.791$ $G_1 = 4.986$ $\tau_2 = 1.241$ $G_2 = 2.149$ $K_p = 2.624$ $K_i = 0.725$ $K_d = 0.439$ $W_p = 2.850$ $W_d = 2.061$
t_s **(s) (2% band)**	Δf_1	20.91	15.69	11.47	8.31	4.38	**2.18**
	Δf_2	20.80	20.05	13.66	6.25	4.51	**3.48**
	ΔP_{tie}	11.54	17.82	12.28	6.51	3.98	**1.98**
J_{ITAE}		1.0566	0.9197	0.3818	0.1557	0.0461	**0.02237**

5. State Space Model of 2-ANRT PS

To perform a detailed analysis of the 2-ANRT PS shown in Fig. 2(b), the full state space model of the system is expressed as follows:

$$\dot{x} = Ax + B_1 u + B_2 \omega \tag{15}$$

Where, x denotes the state variables in Eq. (16), A denoted the state matrix, B_1 and B_2 are the control and disturbance matrix, respectively. u and ω are the control and disturbance variables, respectively.

$$x = \left[\Delta f_1\ \Delta P_{g1}\ \Delta P_{t1}\ \Delta f_2\ \Delta P_{g2}\ \Delta P_{t2}\ \Delta P_{tie}\ \int (ACE_1 - ACE_2)dt\right]^T \tag{16}$$

Where, Δf_1 and Δf_2 are refer to frequency deviations in Area1-2, ΔP_{g1} and ΔP_{g2} are generator output powers, ΔP_{t1} and ΔP_{t2} are turbine output powers, ΔP_{tie} is tie-line power, ACE_1 and ACE_2 are area control errors. The disturbances variables are expressed as follows:

$$\omega = [\Delta P_{L1}\ \Delta P_{L2}]^T \tag{17}$$

Where, ΔP_{L1} and ΔP_{L2} are refer to load deviations in Area1-2. The control variables are expressed as follows:

$$u = [\Delta u_1 \; \Delta u_2 \;]^T \tag{18}$$

Where, Δu_1 and Δu_2 are refer to output of the EXP-2DOF-PID controller in Area1-2.

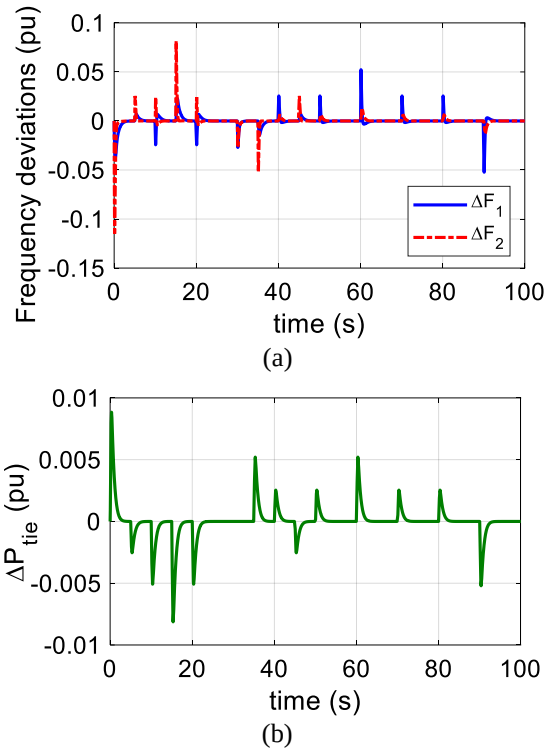

Fig.11. Respectively frequency and tie-line power deviations responses at change load.

6. Conclusion

A new SFS-optimized EXP-2DOF-PID controller is proposed in this work to solve the load frequency control problem in power systems with diverse structures. The EXP function block placed before the 2DOF-PID controller processes the error and its time derivative, combining them to generate a nonlinear error signal. The signal serves as the input to the 2DOF-PID controller. Such a controller design has been proven to have an excellent control strategy. In order to obtain the highest possible performance from the proposed controller, the SFS algorithm is applied to determine the controller parameters values. To highlight the robustness and reliability of the proposed controller, it is applied to 2-area single/multi-source PSs, which are widely used in research on this subject. The pu load change value applied to each PS model is determined to be the same as other studies compared to making a fair comparison. In the tests, the EXP-2DOF-PID controller outperformed all its competitors in relation to error rate and settling time. In the tests, it was seen that the EXP-2DOF-PID controller has better performance than all its competitors in relation to error rate, settling time and it quickly damps even load changes with large oscillations. In real-world power systems, the communication network introduces delays, date losses, and noise in measurement signals due to sensor inaccuracies. These factors can significantly degrade the performance of time-sensitive controllers like 2DOF-PID, especially in wide-area control applications. The current study does not incorporate such practical communication constraints.

Appendix:

- 2-ANRT PS model excluding GDB are [21], [27], [28]; $T_{12} = 0.545$ pu MW/rad, $T_{ps} = 20$ s, $K_{ps} = 120$ Hz/pu, $T_t = 0.3$ s, $T_g = 0.03$ s, $R = 2.4$ Hz/pu, $B = 0.425$ pu MW/Hz, $f_0 = 60$ Hz.

- 2-ANRT PS model with GDB are [21], [28], [29]; $T_{12} = 0.444$ pu MW/rad, $T_{ps} = 20$ s, $K_{ps} = 120$ Hz/pu, $T_t = 0.3$ s, $T_g = 0.2$ s, $R = 2.4$ Hz/pu, $B = 0.425$ pu MW/Hz, $f_0 = 60$ Hz.

- 2-AMS PS model are [21], [30, [32]; $T_{12} = 0.433$ pu MW/rad, $T_{ps} = 11.49$ s, $K_{ps} = 68.9566$ Hz/pu, $T_t = 0.3$ s, $T_{gh} = 0.2$ s, $R = 2.4$ Hz/pu, $B = 0.4312$ pu MW/Hz, $f_0 = 60$ Hz, $T_{sg} = 0.08$ s, $T_r = 10$, $T_{rs} = 5$ s, $T_{rh} = 28.75$ s, $T_{cr} = 0.01$ s, $T_{cd} = 0.5$ s, $T_f = 0.23$ s, $T_w = 1$ s, $b_g = 0.05$ s, $c_g = 1$, $X_c = 0.6$ s, $Y_c = 1$ s, $K_r = 0.3$, $K_T = 0.543478$ pu, $K_H = 0.326084$ pu, $K_G = 0.130438$ pu.

References

[1] R. Choudhary, J. N. Rai and Y. Arya, "Cascade FOPI-FOPTID controller with energy storage devices for AGC performance advancement of electric power systems", Sustainable Energy Technologies and Assessments, vol. 53, Oct. 2022.

[2] S. Das, S. Datta, L. C. Saikia and S. K. Bhagat, "Effect of electric vehicles and TIDN-(1+PI) controller on LFC in hydro-thermal-archimedes wave energy-geothermal-wind generations based multiarea system", Proc. 4th Int. Conf. Energy Power Environ. (ICEPE), pp. 1-6, 2022.

[3] S. Oladipo, Y. Sun and Z. Wang, "Application of a new fusion of flower pollinated with pathfinder algorithm for AGC of multi-source interconnected power system", IEEE Access, vol. 9, pp. 94149-94168, 2021.

[4] X. He, X. Liu and P. Li, "Coordinated false data injection attacks in AGC system and its countermeasure", IEEE Access, vol. 8, pp. 194640-194651, 2020.

[5] R. Sivalingam, S. Chinnamuthu and S. S. Dash, "A hybrid stochastic fractal search and local unimodal sampling based multistage PDF plus (1+PI) controller for automatic generation control of power systems", J. Franklin Inst., vol. 354, no. 12, pp. 4762-4783, 2017.

[6] M. Shirkhani, J. Tavoosi, S. Danyali, A. K. Sarvenoee, A. Abdali, A. Mohammadzadeh, and C. Zhang, "A review on microgrid decentralized energy/voltage

control structures and methods", Energy Reports, 10, pp. 368-380, 2023.

[7] I. F. Davoudkhani, P. Zare, A. Y. Abdelaziz, M. Bajaj, and M.B. Tuka, "Robust load-frequency control of islanded urban microgrid using 1PD-3DOF-PID controller including mobile EV energy storage", Scientific Reports, 14(1), 13962, 2024.

[8] R. Alayi, F. Zishan, S. R. Seyednouri, R. Kumar, M. H. Ahmadi, and M. Sharifpur, "Optimal load frequency control of island microgrids via a PID controller in the presence of wind turbine and PV". Sustainability, vol.13, no. 19, 10728, 2021.

[9] S. Panda, B. Mohanty and P.K. Hota, "Hybrid BFOA–PSO algorithm for automatic generation control of linear and nonlinear interconnected power systems", Applied soft computing, vol. 13, no. 12, pp. 4718-4730, 2013.

[10] D. Yousri, T. S. Babu, and A. Fathy, "Recent methodology based Harris Hawks optimizer for designing load frequency control incorporated in multi-interconnected renewable energy plants", Sustainable Energy, Grids and Networks, 22, 100352, 2020.

[11] E. Çelik, "Improved stochastic fractal search algorithm and modified cost function for automatic generation control of interconnected electric power systems" Engineering Applications of Artificial Intelligence, 88, 2020.

[12] E. Çelik, "Exponential PID controller for effective load frequency regulation of electric power systems", ISA transactions, 153, 364-383, 2024.

[13] S. Padhy, S. Panda, S. Mahapatra "A modified GWO technique based cascade PI-PD controller for AGC of power systems in presence of plug in electric vehicles", Engineering Science and Technology, an International Journal, vol. 20 pp. 427-442, 2017.

[14] P. K. Hota and B. Mohanty, "Automatic generation control of multi source power generation under deregulated environment", Int. J. Electr. Power Energy Syst., vol. 75, pp. 205-214, 2016.

[15] S. Chakraborty, A. Mondal, "TSA-aided IT2FLC-(1+PD)-FOPID control for regulating the first-order plus time-delayed non-conventional multi-area power system with deregulation", Electr Eng (2025).

[16] E. Çelik, N. Öztürk, Y. Arya and C. Ocak, "(1+ PD)-PID cascade controller design for performance betterment of load frequency control in diverse electric power systems", Neural Computing and Applications, vol. 33, no. 22, pp. 15433-15456, 2021.

[17] E. Çelik, "Design of new fractional order PI–fractional order PD cascade controller through dragonfly search algorithm for advanced load frequency control of power systems", Soft. Comput, vol. 25, no. 2, pp. 1193-1217, 2021.

[18] N. C. Patel, M. K. Debnath, D. P. Bagarty, and P. Das, "GWO tuned multi degree of freedom PID controller for load frequency control", International Journal of Engineering & Technology, vol. 7, no. 3.3, pp. 548, 2018.

[19] M. Sariki, and R. Shankar, "Optimal CC-2DOF (PI)-PDF controller for LFC of restructured multi-area power system with IES-based modified HVDC tie-line and electric vehicles", Engineering Science and Technology, an International Journal, 32, 101058, 2022.

[20] Ö. Can, M. Ş. Ayas, and E. Çelik, "Frequency and voltage stability improvement in a two-area thermal power system using a novel controller and RIME optimizer", Computers and Electrical Engineering, vol. 125, 110434, (2025).

[21] E. Çelik, "Improved stochastic fractal search algorithm and modified cost function for automatic generation control of interconnected electric power systems", Engineering Applications of Artificial Intelligence, 88, 103407, 2020.

[22] M. Altahhan, and N. Saha, "Hybrid many optimising Liaison and Harris Hawk optimised double fuzzy PD-PI+ PIDF controller to adjust frequency for the two-area non-reheat system", International Journal of Ambient Energy, vol. 46, no. 1, 2462591, 2025.

[23] S. K. Ojha and M. C. Obaiah, "Optimization of a Novel FOPIDN-(1+ PIDN) controller for Renewable Integrated Multi-Area Load Frequency Control System with Non-linearities". IEEE Access, vol. 13, pp. 56736-56755, 2025.

[24] N. K. Jena, S. Sahoo, K. Kasturi and B. K. Sahu, "Design of a Fractional Order 2-DoF-PID Controller for Frequency Control in a Multi-Area Stand Alone Micro-Grid," 2024 3rd Odisha International Conference on Electrical Power Engineering, Communication and Computing Technology (ODICON), Bhubaneswar, India, pp. 1-6, 2024.

[25] H. Salimi, "Stochastic Fractal Search: A powerful metaheuristic algorithm," Knowl Based Syst, vol. 75, pp. 1–18, Feb. 2015.

[26] A. K. Barisal, "Comparative performance analysis of teaching learning based optimization for automatic load frequency control of multi-source power systems," International Journal of Electrical Power & Energy Systems, vol. 66, pp. 67–77, 2015.

[27] R.K. Sahu, S. Panda, U.K. Rout, D.K. Sahoo, "Teaching learning based optimization algorithm for automatic generation control of power system using 2-DOF PID controller", Int J Electr Power Energy Syst, 77, pp. 287-301, 2016.

[28] R.K. Sahu, S. Panda, G.T.C. Sekhar," A novel hybrid PSO-PS optimized fuzzy PI controller for AGC in multi area interconnected power systems", Int J Electr Power Energy Syst, 64, pp. 880-893, 2015.

[29] B. Mohanty, S. Panda, P.K. Hota," Differential evolution algorithm based automatic generation control for interconnected power systems with non-linearity", Alex Eng J, vol. 53, pp. 537-552, 2014.

[30] B. Mohanty, S. Panda, P.K. Hota, "Controller parameters tuning of differential evolution algorithm and its application to load frequency control of multi-source power system", Int J Electr Power Energy Syst, vol. 54, pp. 77-85, 2014.

[31] R.K. Khadanga, A. Kumar, S. Panda, "A modified grey wolf optimization with cuckoo search algorithm for load frequency controller design of hybrid power system", Appl Soft Comput, 124, Article 109011, 2022.

[32] S. Padhy, S. Panda, "A hybrid stochastic fractal search and pattern search technique based cascade PI-PD controller for automatic generation control of multi-source power systems in presence of plug in electric vehicles", Appl Soft Comput, 124, Article 109011, 2022.